

# SETUP FOR HIGH-TEMPERATURE PROCESSING OF SILICON CARBIDE

# Andrzej KUBIAK

 $Lodz\ University\ of\ Technology,\ Department\ of\ Semiconductor\ and\ Optoelectronic\ Devices,\ 93-590\ Lodz,\ Poland,\ andrzej.kubiak@p.lodz.pl$ 

DOI: https://doi.org/10.24136/jaeee.2025.013

**Abstract:** – This work outlines the conditions and requirements for high-temperature processes used in the fabrication of silicon carbide based semiconductor structures. A dedicated setup was developed by adapting the VLS10/18 system to perform thermal processes at temperatures exceeding 2000°C. Comprehensive characterization confirmed the system's ability to maintain controlled conditions suitable for post-implantation annealing and thermal diffusion of dopants in monocrystalline SiC. The study also verified the accuracy of pyrometric temperature measurements and examined the heating and cooling dynamics of the reactor.

Keywords – annealing, doping, pyrometric measurement, thermal processing, silicon carbide

### INTRODUCTION

A distinctive feature of the technology used for manufacturing semiconductor devices based on silicon carbide (SiC) is the requirement for thermal processes to be conducted at significantly higher temperatures than those used in conventional silicon-based technologies. This presents a considerable technical challenge, as equipment with quartz reactors – commonly used in silicon processing – cannot be directly applied due to the temperature dependent flow behavior of the quartz, which becomes problematic at elevated temperatures. In SiC processing, epitaxial layer growth typically requires temperatures between 1450–1650°C. Post-implantation annealing processes are carried out at 1500–1700°C, while thermal diffusion doping requires temperatures exceeding 1800°C [1-5]. Such extreme temperatures surpass the limits of many materials used in the reactor construction for silicon technologies. In practice, the only materials that can reliably withstand these conditions are carbon-based. Including graphite and its derivatives, such as thermally insulating carbon fiber felt.

In recent years, various attempts have been made to adapt high-temperature equipment originally designed for silicon technology to the requirements of SiC processing. Efforts have also focused on modifying such systems to achieve the necessary temperature ranges. The first

purpose-built systems for SiC device fabrication were epitaxial reactors capable of operating at 1600–1800°C, typically employing graphite process chambers. For post-implantation annealing, electrothermal systems from other fields have been adapted. These systems directly heat the processed component itself, producing a momentary local temperature rise while maintaining the surrounding system components at safe operating levels. This effect can be achieved through several techniques, including the absorption of radiation from a focused laser radiation [6] or halogen lamps [7], exposure to a high-power plasma jet [8], RF-induced self-heating [9], or microvawe-generated fields [10].

To ensure effective annealing of silicon carbide substrates in high-temperature furnaces, the experimental setup must satisfy the following conditions:

- · capability of reaching and precisely controlling temperatures up to 2000°C,
- uniform temperature distribution within the reactor to prevent parasitic sublimation or unintended SiC epitaxy during annealing,
  - reactor construction using materials chemically inert to SiC (e.g., graphite),
- vacuum-tight design equipped with a pumping system to eliminate gaseous contaminants before processing and maintain high process purity,
  - integrated gas delivery system (e.g., argon, nitrogen) and pressure measurement capability.

## 1 DESIGN AND ADAPTATION OF THE VLS10/18 FURNACE

Based on above requirements, an optimal solution for high-temperature silicon carbide processing is the use of a vacuum furnace equipped with a graphite reactor and a high-power heating system. These criteria are largely met by the VLS10/18 industrial furnace, available in the technological laboratory of the Department of Semiconductor and Optoelectronic Devices at Lodz University of Technology.

Originally designed for sintering, annealing, brazing, and melting materials under both reduced and elevated pressure, the furnace is equipped with a 20 kW power supply, a vacuum system comprising a low-vacuum rotary pump and a high-vacuum diffusion pump, a liquid cooling system, a reactor chamber with a volume of approximately 20 liters. The base of the reactor also functions as an electrical feedthrough for interchangeable heating elements. Temperature measurement is possible using either a thermocouple or optical methods, the latter via a dedicated quartz window. Chamber pressure is monitored using standard vacuum gauge heads.

The furnace accommodates heating elements made from materials such as molybdenum, chromo-nickel alloys, graphite, tantalum, or tungsten, allowing a range of maximum operating temperatures. When equipped with a graphite reactor, the system can reach temperatures up to 2200°C, which is sufficient for all high-temperature processes required in SiC technology.

These characteristics make the furnace a strong candidate for modification as a reliable and efficient tool for SiC device processing. Figure 1 presents a schematic of the furnace, with proposed modifications highlighted in red to enable safe and precisely controlled high-temperature SiC processing. These modifications include:

- · a closed graphite cassette for processing SiC in a controlled ambient atmosphere,
- · non-invasive temperature measurement,
- integrated pressure measurement.

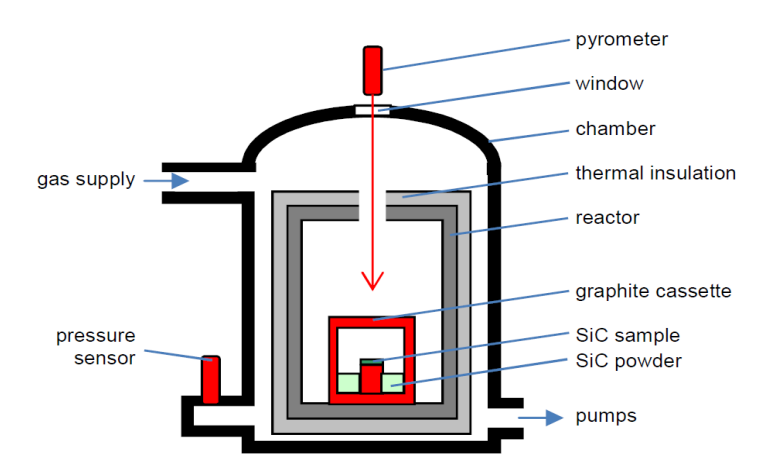


Fig. 1. Scheme of the VLS10/18 furnace; red-marked are the introduced modifications

#### **2** GRAPHITE CASSETTES

An essential component of the furnace modification involved the design and fabrication of custom closed graphite cassettes, which are placed inside the reactor chamber. These cassettes, fabricated from the same type of graphite used in the construction of the VLS10/18 furnace reactor ensuring material compatibility and thermal stability, enable the controlled annealing of SiC substrates in an inert protective atmosphere. One example, shown in Figure 2a, has a cylindrical shape with a diameter of 40 mm, a height of 35 mm, and a wall thickness of 5 mm.

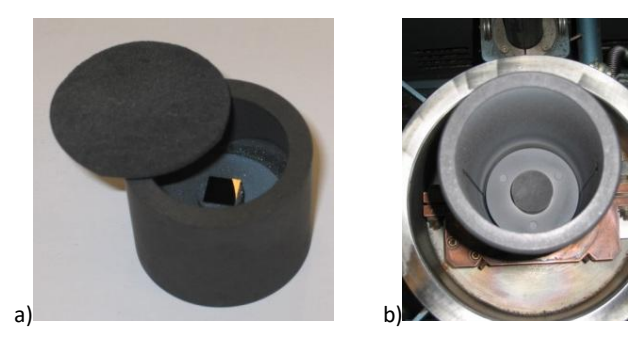


Fig. 2. Cassette with SiC substrate and powdered SiC (a) and its location in the reactor (b)

A SiC sample, typically measuring approximately  $10 \times 10$  mm, can be placed in the central part of the cassette and surrounded by a substantial volume of powdered silicon carbide. This powder may optionally be mixed with a doping source, such as boron or phosphorus. During the heating process, the SiC powder acts as an additional source of volatile species, including Si, Si2C, SiC2, and C. By saturating the surrounding atmosphere, these species effectively reduce the sublimation of silicon from the surface of the SiC sample. For annealing and thermal diffusion processes, the loaded cassette is positioned inside the furnace reactor, as illustrated in Figure 2b.

The use of an additional graphite cassette, in which the heated SiC samples can be placed, makes temperature control of processed SiC substrates difficult, since their temperature cannot be measured directly. As the monitoring of the SiC sample temperature is critically important for proper process flow, an indirect method involving the use of the CAD approach has been developed and verified [11]. A numerical model of a furnace reactor was created on the basis of the commercial ANSYS package, allowing for the simulation of thermal fields under given heat-dissipation conditions in the modeled area and in the presence of gaseous and liquid media participating in heat exchange and transport. The model acts as an accurate tool for temperature distribution verification during the high-temperature annealing of and diffusion of dopants for silicon carbide.

Example of the temperature field distribution inside the furnace chamber and graphite cassette is presented on Figure 3.

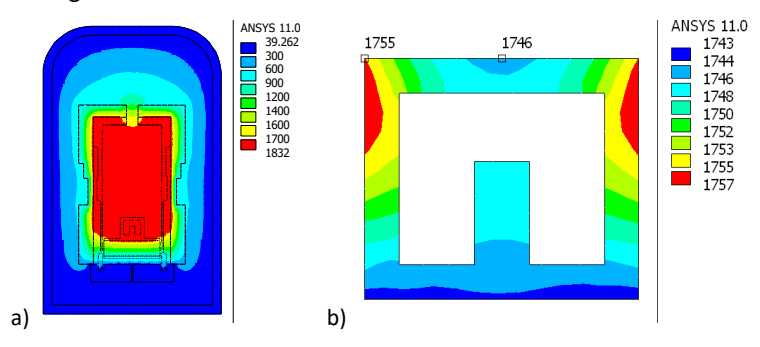


Fig. 3. Example of the temperature distribution in the ANSYS model of the VLS 10/18 furnace (a) and the graphite cassette (b) [11]

# 3 Non-invasive Temperature Measurement

Precise temperature control during the annealing of SiC is a critical aspect of the heating process. These processes require relatively high temperatures and are conducted in a closed graphite crucible, which makes the use of direct-contact temperature sensors, such as thermocouples, impractical.

However, the furnace design includes a quartz glass window located in its upper section, allowing visual observation of the reactor interior during heating. This feature enabled the implementation of an optical pyrometer, which complements the standard thermocouple typically inserted from the bottom of the reactor in conventional VLS10/18 furnace applications. Pyrometric temperature control is a well-established method for temperature monitoring in closed reactors during semiconductor processing [12].

For this purpose, a Raytek MR1SC pyrometer was employed, with its specifications listed in Table 1. The device was permanently mounted in the upper section of the furnace, enabling temperature monitoring of the reactor interior through the quartz window and an aperture in the center of the heater cover. To ensure accurate readings through the quartz glass, the pyrometer was operated in a two-spectral-range mode.

To determine the emissivity (grayness coefficient) of the graphite reactor in the furnace,

a diffusion furnace was used as a reference device during the calibration process. The temperature in the diffusion furnace was monitored using tungsten-rhenium thermocouples and stabilized with an accuracy of ±0,5°C. A graphite element taken from the modified furnace was placed inside the quartz reactor of the diffusion furnace, under a protective nitrogen atmosphere and at a fixed, controlled temperature. The optical pyrometer was then aimed at the heated graphite element, and the emissivity setting (slope) was adjusted until the pyrometric reading matched the known reference temperature from the diffusion furnace. Calibration was performed at two temperature points: 1000°C, which is the minimum measurable temperature for the pyrometer, and 1350°C, corresponding to the maximum operating temperature of the diffusion furnace. In both cases, the same emissivity value of 0,989 was obtained, confirming the consistency of the material's radiative properties in this range.

Table 1. Raytek R1SC pyrometer parameters

made pyromotor parameters	
Parameter	Value
temperature range	10003000ºC
measurement accuracy	±0,75%
optical resolution	130:1
spectral range	0,751,1μm

## 4 PRESSURE MEASUREMENT

To facilitate heat conduction and dopant diffusion processes in SiC substrates, it is essential to maintain not only precise temperature control but also a neutral gas atmosphere with accurately regulated pressure. To this end, an adaptive gas supply system was developed, featuring a controllable dosing valve and an integrated pressure measurement system within the reactor chamber. The constructed gas installation operates with argon of 5,0 purity, delivered to the reactor chamber via a ZDA-2 dosing valve. This valve enables gas flow regulation within the range of 0,01 to 100 mbar\*I/s (approximately 0,6 to 6000 sccm).

The pressure measurement system in the furnace's working chamber is based on the Leybold Center Three three-way vacuum gauge. It includes two low-vacuum channels (Thermovac TTR 91 probes) and one high-vacuum channel (Penning PTR 225 probe). The Thermovac probes measure pressure from  $5\times10$ -4 to  $1\times103$  mbar, with optimal accuracy ( $\pm15\%$  of the reading) maintained between  $1\times10$ -3 and 100 mbar. The Penning probe covers a range from  $1\times10$ -9 to  $1\times10$ -2 mbar, with an accuracy of  $\pm30\%$  of the reading. This setup enables pressure monitoring throughout the heating process, from atmospheric pressure down to  $1\times10$ -9 mbar, fully meeting the requirements of the conducted experiments.

# 5 CHARACTERIZATION OF THE FURNACE

Prior to the planned high-temperature processing of silicon carbide substrates, a series of tests were carried out to evaluate the furnace's thermal performance under various operating conditions. The primary objective was to establish the relationship between the electrical power supplied at a given pressure in the reactor chamber and the resulting temperature distribution within the working area, both under static and dynamic operating conditions. Argon was used

as the working gas to fill the reactor chamber during the tests. The study involved a series of heating cycles conducted under different parameters, with the following goals:

- to determine the temperature characteristics of the furnace as a function of power,
- to assess the effect of pressure variations on the steady-state temperature for a given power input,
  - to evaluate the heating and cooling dynamics of the system,
- to independently verify temperature readings obtained pyrometrically on the top surface of the closed graphite cassette.

All tests were conducted in a configuration when a closed graphite cassette was placed inside the furnace reactor, with the temperature pyrometrically measured on the upper surface of the cassette.

#### 5.1 TEMPERATURE CHARACTERISTICS

To determine the relationship between the supplied electrical power and the temperature on the upper surface of a graphite cassette placed inside the reactor under steady-state conditions, a series of controlled heating tests were performed. These tests were conducted at constant power levels ranging from 5 to 15 kW, regulated by monitoring current and voltage values. All temperature measurements were taken using the optical pyrometer operating in a two-spectral-range mode. Due to the device's limitations, temperature profiles were recorded only for values above 1000 °C. The heating experiments were carried out in an argon atmosphere, with the reactor chamber pressure maintained at 10 Pa.

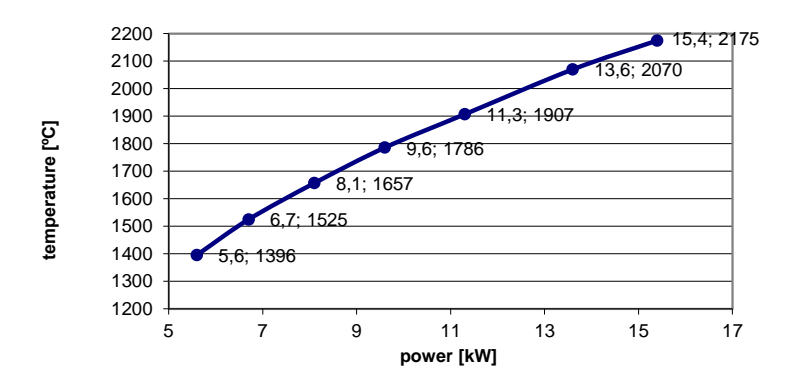


Fig. 4. Dependence of the temperature in the thermally steady state as a function of the supplied electric power at 10 Pa

The correlation between the supplied power and the steady-state temperature inside the reactor is presented in Figure 4. This characteristic served as the basis for preliminary calibration of the furnace and helped establish a functional relationship between delivered power and the resulting steady-state temperature. The results show that, when using a graphite heating element, achieving temperatures in the range of 1800–2000 °C requires a power input of approximately 10 to 13 kW. At 15.4 kW, a temperature of 2175 °C was reached—approaching the maximum permissible operating temperature for the graphite heating element, defined as 2200 °C. The furnace is capable of delivering up to 20 kW of heating power. This capacity enables

the use of a specialized heating element made of tantalum, which allows for operating temperatures of up to 2800 °C. However, such high temperatures exceed the requirements of the experiments conducted on silicon carbide substrates.

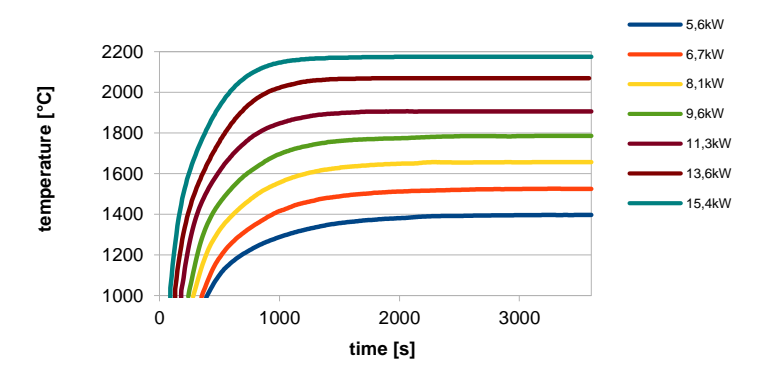


Fig. 5. The heating process of the furnace reactor for different values of power supplied at a pressure of 10 Pa

For selected power supply levels, temperature profiles over time were recorded, as shown in Figure 5. The results indicate that, under constant power conditions, the furnace reaches thermal steady state approximately 50 minutes after surpassing 1000 °C. This corresponds to a total heating period of about one hour starting from room temperature. The heating dynamics is limited by the current capacity of the power supply, and its further increase would pose a risk of damaging the heating element due to stresses caused by the thermal expansion.

# **5.2** EFFECT OF PRESSURE CHANGES

The effect of working atmosphere pressure on the steady-state temperature was investigated at a constant power supply of 9 kW. Again, pyrometric temperature measurements were taken on the upper surface of the graphite cassette inside the furnace reactor. The experiment began with a 3-hour heating stage conducted at the lowest achievable pressure of 0,04 Pa, attained using the furnace's vacuum system. Under these conditions, the system reached an initial thermal steady state, corresponding to a temperature of 1736 °C in the upper surface of a graphite cassette placed inside the reactor. Following this, the pressure was gradually increased by controlled argon flow. The first adjustment raised the pressure to 0,1 Pa, after which pyrometer readings were recorded. Subsequently, the pressure was increased stepwise every 30 minutes to 1 Pa, 10 Pa, 100 Pa, and finally 1000 Pa. The results of this experiment are presented in Figure 6, where the temperature profile over time is shown, with the corresponding argon pressure changes clearly marked.

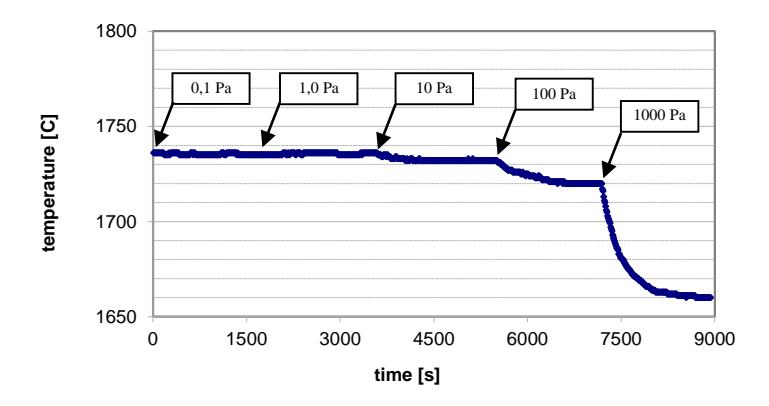


Fig. 6. Influence of gas pressure on the furnace temperature (9 kW, pressure increments every 30 minutes are marked)

The results indicate that, within the pressure range of 0,1 Pa to 1,0 Pa, the presence of working gas has no significant effect on the temperature in the furnace's working chamber. At such low pressures, the amount of gas present is insufficient to meaningfully contribute to heat transfer between furnace components. However, this changes as the pressure increases. At 10 Pa, a temperature decrease of approximately 3°C is observed. At 100 Pa, the temperature drop reaches 14°C, and at 1000 Pa, it increases significantly to 75°C. These reductions are attributed to enhanced convective and conductive heat losses due to the increased gas density. Further pressure increases led to pronounced heating of the upper part of the furnace chamber, suggesting excessive heat accumulation in areas not monitored by the primary temperature sensors. As a result, measurements at higher pressures were not conducted for safety and system stability reasons.

To further characterize the relationship between furnace temperature in a thermally steady state and the working gas pressure, additional heating experiments were conducted at selected power levels: 5.6 kW and 11.3 kW.

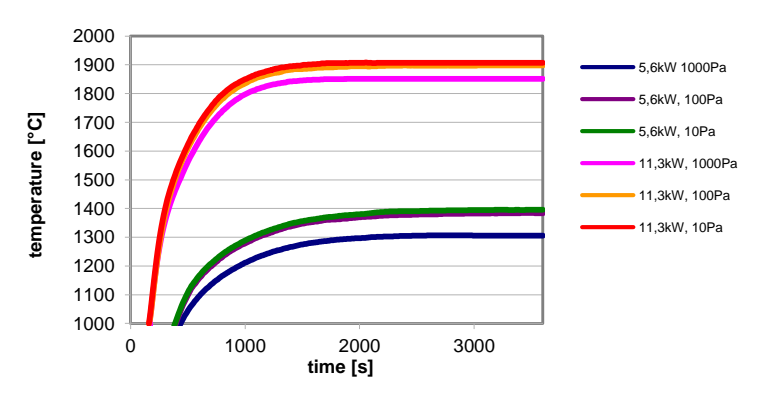


Fig. 7. Working gas pressure influence on the temperature for the power 5,6 kW and 11,3 kW

During these tests, the pressure in the reactor chamber was maintained at 10, 100, and 1000 Pa. The resulting temperature characteristics are presented in Figure 7. For each power level, the highest temperatures were recorded at the lowest working gas pressure. As pressure increases, enhanced heat transfer occurs within the reactor, primarily through convection. This leads to increased heat flow from the heating element to the cooler components, such as the chamber walls, resulting in lower measured temperatures in the working zone.

#### 6 HEATING AND COOLING DYNAMICS

The thermal characteristics presented in Figure 4 show that, under constant power supply, the furnace heating time is relatively long – up to one hour. This extended duration is undesirable, as it limits precise control over maintaining the test sample at the target temperature. Given that the power supply exceeds the requirements for sustaining temperatures up to 2000°C, additional tests were carried out to reduce heating time by implementing a two-stage energy delivery approach. In this method, maximum available power is applied during the initial heating phase to accelerate temperature rise, followed by a reduction to the necessary power level for maintaining the desired temperature during the stabilization phase.

In the first stage, the minimum time required to heat the reactor from room temperature to target temperatures of 1300°C, 1500°C, 1700°C, 1800°C, 1900°C, and 2000°C was determined. To achieve this, heating was performed using the maximum available power supply of 20 kW. Throughout the experiment, the reactor was maintained in an argon atmosphere at a pressure of 10 Pa. Temperature measurements on the upper surface of the graphite cassette inside the reactor were taken using a pyrometer. The results of these measurements are summarized in Table 2.

Table 2. Furnace heating time required to reach the target temperature from RT at 20 kW power

Temperature [°C]	Time [s]
1300	130
1500	170
1700	230
1800	280
1900	340
2000	420

Based on the data from Table 2 and the steady-state temperature versus supplied electrical power relationship shown in Figure 4, test heating profiles were designed and verified for target temperatures from 1300°C to 2000°C. The experiments were carried out in an argon atmosphere at a pressure of 10 Pa. Each thermal cycle consisted of three stages: heating, temperature maintenance, and cooling. The resulting temperature profiles are presented in Figure 8. Due to the pyrometer's measurement limitations, only temperatures exceeding 1000°C were recorded and analyzed.

During the heating stage, electrical power of 20 kW was supplied to the reactor to achieve the highest possible heating rate (t1). Once the target temperature was reached, the power was reduced to a level sufficient to maintain thermal stabilization (t2), which was held constant for 10 minutes in each process. After the stabilization period, the furnace power supply was turned off to enable the fastest possible cooling to room temperature (t3).

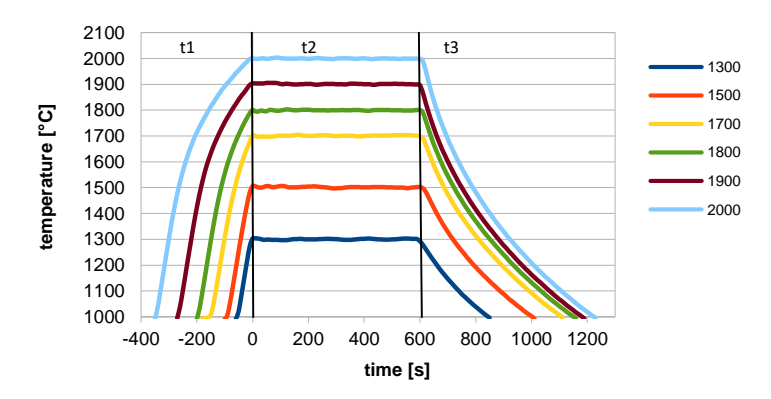


Fig. 8. Thermal profiles obtained for selected temperature levels at 10 Pa

Based on the slopes of the temperature profiles during the heating and cooling phases, the dynamics of these processes were estimated. During the heating stage at the selected power level, the temperature increase rate varied from approximately  $360^{\circ}\text{C/min}$  for lower temperature ranges ( $1000^{\circ}\text{C}$  to  $1300^{\circ}\text{C}$ ) to about  $66^{\circ}\text{C/min}$  for higher ranges ( $1800^{\circ}\text{C}$  to  $2000^{\circ}\text{C}$ ). During cooling, the temperature decrease rate ranged from roughly  $100^{\circ}\text{C/min}$  (cooling from  $1300^{\circ}\text{C}$  to  $1000^{\circ}\text{C}$ ) up to  $200^{\circ}\text{C/min}$  (cooling from  $2000^{\circ}\text{C}$  to  $1800^{\circ}\text{C}$ ).

The proposed approach significantly shortened the heating stage duration to just a few minutes, which is adequate for typical SiC substrate heating processes that require maintaining the set temperature for several tens of minutes. Considering the negligible effect of working gas at pressures below 100 Pa on heat transfer within the reactor, it can be assumed that heating processes conducted at pressures between 1 Pa and 100 Pa will exhibit similar heating and cooling rate profiles.

# 7 VERIFICATION OF THE CASSETTE'S TEMPERATURE

The achievement and verification of the target temperatures in the reactor were confirmed through a series of experimental tests involving the heating of a material with a well-known melting point. Silicon was chosen for this purpose, with a melting temperature of 1412°C. Several heating cycles were performed at set temperatures of 1400, 1405, 1410, 1415, and 1420°C, each maintained for 20 minutes. In each experiment, a piece of monocrystalline silicon wafer was placed on the upper surface of the graphite cassette (as shown in Figure 2a), which was positioned inside the reactor as illustrated in Figure 2b.

The experiment demonstrated that melting of the monocrystalline silicon did not occur at a pyrometrically measured temperature of 1415°C, but was observed after annealing the sample at 1420°C. These results allowed for estimating the accuracy of the pyrometer-based temperature measurements to be within ±10°C, corresponding to a measurement error of approximately 0,7%. This level of accuracy is acceptable for the silicon carbide processing applications under consideration.

#### 8 CONCLUSIONS

This paper presents the adaptation of the VLS10/18 furnace for high-temperature processing of silicon carbide. Characterization of the furnace's thermal parameters confirmed its capability to operate steadily at temperatures up to 2000°C, which are essential for SiC processing. High-temperature operations can be conducted under variable pressures, supported by precise temperature measurements of the graphite cassette positioned inside the reactor. Additionally, heating and cooling rates were verified, alongside the accuracy of pyrometric temperature measurements.

The completed work has demonstrated that the constructed setup enables effective research on post-implantation annealing and thermal diffusion of dopants in silicon carbide, making it a valuable tool for the fabrication of semiconductor structures in SiC.

#### **BIBLIOGRAPHY**

- [1] Mokhov E. N. (2019) "Doping of SiC Crystals during Sublimation Growth and Diffusion". In: Crystal Growth, InTechOpen, Rijeka, http://dx.doi.org/10.5772/intechopen.82346
- [2] Pelleg, J. (2016). "Diffusion in Silicon Carbide (Carborundum)". In: Diffusion in Ceramics. Solid Mechanics and Its Applications, vol. 221 Springer, <a href="http://doi.org/10.1007/978-3-319-18437-12">http://doi.org/10.1007/978-3-319-18437-12</a>
- [3] Zippelius B.; Suda J; Kimoto T. (2012) "High temperature annealing of n-type 4H-SiC: Impact on intrinsic defects and carrier lifetime" J. Appl. Phys. 111, 033515, https://doi.org/10.1063/1.3681806
- [4] Roccaforte, F.; Fiorenza, P.; Vivona, M.; Greco, G.; Giannazzo, F. (2021) "Selective Doping in Silicon Carbide Power Devices". Materials, 14, 3923, <a href="https://doi.org/10.3390/ma14143923">https://doi.org/10.3390/ma14143923</a>
- [5] Kamiński, M.; Król, K.; Kwietniewski, N.; Myśliwiec, M.; Sochacki et al. (2025) "The Overview of Silicon Carbide Technology: Status, Challenges, Key Drivers, and Product Roadmap". Materials, 18, 12, <a href="https://doi.org/10.3390/ma18010012">https://doi.org/10.3390/ma18010012</a>
- [6] Calabretta, C.; Agati, M.; Zimbone, M.; Boninelli, S.; Castiello et al. (2019) "Laser Annealing of P and Al Implanted 4H-SiC Epitaxial Layers". Materials, 12, 3362, https://doi.org/10.3390/ma12203362
- [7] Zekentes, K.; Vasilevskiy, K. (2020) "Advancing Silicon Carbide Electronics Technology II Core Technologies of Silicon Carbide Device Processing". Materials Research Forum LLC: Millersville, PA, USA; ISBN 978-1-64490-066-6, http://10.21741/9781644900673
- [8] Rambach, M.; Bauer, A.J.; Ryssel, H. (2008) "Electrical and topographical characterization of aluminum implanted layers in 4H silicon carbide". Phys. Status Solidi B, 245, 1315–1326, https://doi.org/10.1002/pssb.200743510

- [9] Zhang, S.; Fu, H.; Li, T.; Fan, G.; Zhao, L. (2023) "Study of Effect of Coil Movement on Growth Conditions of SiC Crystal". Materials 16, 281, https://doi.org/10.3390/ma16010281
- [10] Cichoň S.; Macháč P.; Fekete L.; Lapčák L. (2016) "Direct microwave annealing of SiC substrate for rapid synthesis of quality epitaxial graphene", Carbon Volume 98, 2016, Pages 441-448, ISSN 0008-6223, <a href="https://doi.org/10.1016/j.carbon.2015.11.023">https://doi.org/10.1016/j.carbon.2015.11.023</a>
- [11] Kubiak, A.; Lisik, Z; Raj, E. (2022) "CAD Approach to Control High-Temperature Processes in SiC Technology". Electronics, 11, 768, <a href="https://doi.org/10.3390/electronics11050768">https://doi.org/10.3390/electronics11050768</a>
- [12] Pokryszka P.; Wośko M.; Paszkiewicz R. (2019) "Pomiary in-situ jednorodności temperatury i ex-situ grubości osadzonej warstwy w systemie epitaksjalnym AIXTRON CCS 3 x 2", Przegląd Elektrotechniczny, ISSN 0033-2097, r 95, nr 10/2019, <a href="http://pdoi:10.15199/48.2019.10.40">http://pdoi:10.15199/48.2019.10.40</a>